Solar-Terrestrial Physics. 2024. Vol. 10. Iss. 4. P. 106–113. DOI: 10.12737/stp-104202412. © 2024
Sakharov Ya.A., Yagova N.V., Pilipenko V.A., O.I. Yagodkina, S.L. Garanin. Published by INFRA-M Academic Publishing House

DOI: 10.12737/stp-104202412

Received June 21, 2024
Accepted August 19, 2024

SPATIAL DISTRIBUTION OF AURORAL PRECIPITATION AND FAILURES IN RAILWAY AUTOMATICS AT THE NORTH OF EUROPEAN RUSSIA

Ya.A. Sakharov
Polar Geophysical Institute,
Apatity, Russia, sakharov@pgia.ru
Geophysical Center RAS,
Moscow, Russia

N.V. Yagova
Geophysical Center RAS,
Moscow, Russia, nyagova@ifz.ru
Schmidt Institute of Physics of the Earth RAS,
Moscow, Russia

V.A. Pilipenko
Geophysical Center RAS,
Moscow, Russia, pilipenko_va@mail.ru
Schmidt Institute of Physics of the Earth RAS,
Moscow, Russia

O.I. Yagodkina
Polar Geophysical Institute,
Apatity, Russia, yagodkina@pgia.ru

S.L. Garanin
Vernadsky Institute of Geochemistry and Analytical Chemistry of RAS,
Moscow, Russia, lvovi4s@icloud.com

Abstract. We study the relationship between space weather disturbances and spatial distribution of failures in railway automatics at segments of Northern and October railways in 2001–2006. During the most intensive magnetic storms that caused numerous failures, latitude distribution of auroral electron precipitation and local geomagnetic disturbance, determined as mean absolute value of time derivative of the geomagnetic field horizontal component $|dB_H/dt|$, are examined. We show that in magnetic storm main and recovery phases the segments, where the failures were recorded, correspond to the region of intense auroral precipitation and $|dB_H/dt|$ exceeded 5 nT/s. The relationship between position of auroral oval equatorial boundary and spatial distribution of failures is analyzed for individual magnetic storms and statistically for five years of observations. Both individual cases and statistic tests show that southward displacement of the auroral oval equatorial boundary correlates with increase in the proportion of failures at lower latitude railway segments.

Keywords: space weather, magnetic storms, auroral oval, railways.

INTRODUCTION

The most comprehensive review dealing with the impact of space weather on railway transportation [Pilipenko et al., 2023] provides details of the direct and indirect mechanisms of the effect of disturbances of various types on railway automatics, communication and navigation systems. Although the earliest railway failures related to magnetic storms were recorded more than a century ago [Love et al., 2019], the problem is still topical.

The impact of space weather disturbances on communication and navigation depends significantly on the underlying physical mechanisms; and for wave electromagnetic devices, on frequency as well. Thus, the impact of space weather on these devices changes as technologies advance. Yet, there are also unavoidable effects of space weather disturbances. They are associated with geomagnetically induced currents (GICs), which are excited by geomagnetic field variations in ground-based conductors.

With the same parameters of external disturbances, GIC is greater, the larger the effective area of the circuit in which the electromotive force is induced (currents in the earth's crust are distributed, so we can only conditionally talk about the circuit). The height of the circuit depends on the specific frequency of the process and on the earth's crust conductivity, i.e. it is set by natural parameters; and the length, by the length of the conductor. As a result, the most intense GICs occur in long conductors such as electric power lines, pipelines, and rails.

GIC is an additional quasi-static current, which, when combined with the signaling current of a railway circuit, can cause failures in the automatics responsible for block occupancy. Boteler [2021] by modeling the GIC impact on railway automatics has concluded that the asymmetry of the railway circuit enhances the GIC impact on electrified railways with one electrically continuous rail. Estimates made for the UK railways show that the maximum risks of failures in railway automatics are associated with severe magnetic storms [Patterson et al., 2023a], and the threshold electrotelluric field is lower for the most dangerous failure when a permissive signal occurs at an occupied block [Patterson et al., 2023b].

Study of failures in automatics on the Northern Railway during the most severe magnetic storms (superstorms) has shown [Eroshenko et al., 2010] that each storm is a source of numerous failures at subauroral latitudes. Studying failures in railway automatics on the East Siberian Railway has revealed that at middle geomagnetic latitudes the probability of failures increases many times during strong geomagnetic disturbances [Kasinsky et al., 2007; Ptitsyna et al., 2008]. Active industrial development of the Russian Arctic increases

the risks associated with rare events and raises the question about the reliability of the transport infrastructure during such disturbances.

GICs with the highest amplitude occur in the auroral oval [Beggan, 2015]. During moderate disturbances, the oval equatorial boundary is at geomagnetic latitudes above 65° (auroral latitudes), and during strong disturbances it shifts to lower latitudes. In European Russia, rather long segments of the October and Northern railways are located at auroral latitudes. For these segments, the risk associated with GICs arises already during moderate disturbances. On lower-latitude segments of these railways and on all high-latitude feeders in eastern regions, strong geomagnetic disturbances with intense GICs recorded at subauroral (~60°) and middle geomagnetic latitudes are dangerous.

The GIC intensity depends not only on the auroral electrojet, but also on geomagnetic pulsations and vortex structures [Viljanen et al., 2006; Wik et al., 2008; Wintoft et al., 2016; Sakharov et al., 2021]. At the same time, localization of the most intense GICs is largely determined by the auroral oval position. This poses a question about quantitative description of the relationship between the spatial distribution of failures and the auroral oval position.

The first solutions to the problem of determining the auroral oval position from geomagnetic activity indices, solar wind (SW) plasma and interplanetary magnetic field (IMF) parameters were obtained in the 1960–70s [Feldstein, 1963]. The spatial distribution of auroral electron precipitation has been studied in detail in a series of works performed at the Polar Geophysical Institute [Vorobjev et al., 2000, Vorobjev, Yagodkina, 2005]. These studies resulted in an empirical precipitation model [Vorobjev et al., 2013].

Analysis of ionospheric satellite data made it possible to develop widely used models of precipitation boundaries [Newell et al., 2002]. Existing auroral precipitation models are refined, new models are developed, and new works appear [Milan, 2009; Hu et al., 2017; Chisham et al., 2022]. Since the oval position and the precipitation intensity are important for applications, papers are published which predict precipitation parameters [Ohma et al., 2024], in particular with use of machine learning methods [Hu et al., 2021].

Nevertheless, for many problems the oval equatorial boundary position is described with sufficient accuracy by simple ratios obtained in pioneer works. In a first approximation, the oval equatorial boundary can be represented as a circle with the center shifted to midnight from the geomagnetic pole and a radius determined by the Akasofu parameter [Akasofu, 1979] and the ring current intensity [Milan, 2009].

Statistical studies of the impact of space weather on railway infrastructure are limited by the low availability of data on failures. Recent data is almost unavailable for open research, and earlier data is not unified and not always digitized. As a result, most works on failures in railway automatics are based on modeling, whereas a small number of publications are devoted to data analysis [Kasinskii et al., 2007; Ptitsyna et al., 2008; Wik et al., 2009; Eroshenko et al., 2010].

This study is sequel of the paper [Yagova et al., 2023] dealing with the relationship between the frequency of failures in the October Railway segment lying at auroral latitudes (hereinafter referred to as the auroral segment) and geomagnetic activity on different spatial and temporal scales. In this paper, we examine the relationship between the auroral oval position and the spatial distribution of failures both for individual strong disturbances and in statistics.

1. DATA AND PROCESSING

We analyze the period from 2001 to 2006, which covers the maximum and declining phases of solar cycle 23. The analysis uses the Letneozersky—Shestiozersky segment of the Northern Railway and two segments of the October Railway: Murmansk—Kandalaksha and Belomorsk—Medvezhya Gora (Figure 1).

For case studies, we have selected severe magnetic storms during which failures with no obvious external causes were recorded on the Northern Railway [Eroshenko et al., 2010]. Each of the storms caused failures at geographic latitudes below 64°, which corresponds to geomagnetic latitudes $\Phi<60°$, i.e. to the subauroral zone. This paper examines the spatial distribution of auroral precipitation during these storms. To characterize the precipitation, we use the auroral electron energy flux density J_E, determined by the model [Vorobjev et al., 2013] for the corresponding longitude sector. We estimate the local geomagnetic field disturbance from the Karpogory (KPG) magnetic station's data. Table lists names and codes of the stations, shown in Figure 1, and the magnetometric station KPG, their geographic and Corrected GeoMagnetic (CGM) coordinates, and universal time (UT) of the local magnetic midnight.

For each storm, we analyze the interplanetary medium parameters that most strongly affect geomagnetic activity: IMF components B_z and B_y, SW velocity and dynamic

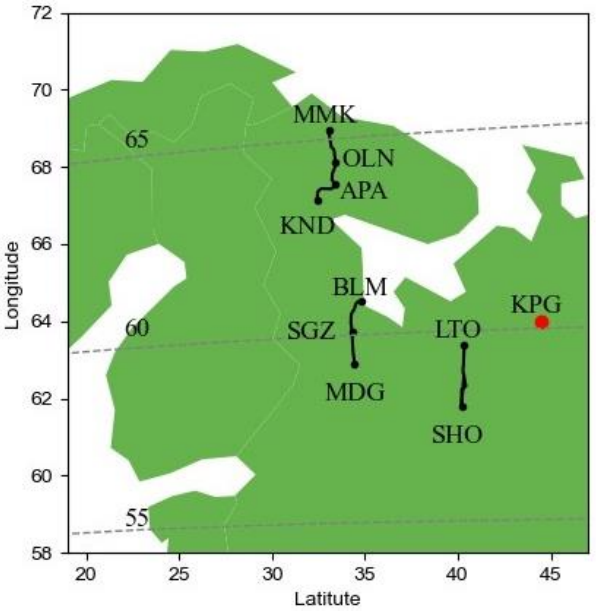

Figure 1. Layout of the Karpogory magnetic station and segments of the October (MMK–KND and BLM–MDG) and Northern (LTO–SHO) railways. Dashed lines are geomagnetic parallels

pressure. To assess global and local geomagnetic activity, we employ the magnetic storm intensity index *Dst* and geomagnetic field variations at KPG respectively; to describe auroral precipitation, the latitudinal distribution of the auroral electron energy flux J_E. Statistical analysis is based on data on failures on two October Railway segments both during magnetic storms and without a storm. The hypothesis about the relationship between the auroral oval equatorial boundary position and the relative frequency of failures on the auroral and subauroral segments is statistically tested.

2. RESULTS

2.1. Case study

The April 11, 2001 magnetic storm began with an increase in the SW velocity V by ~100 km/s for two hours. Figure 2, *a* shows that to 13 UT V<500 km/s, and after 15 UT V>600 km/s. In this mode, the accelerated SW stream catches up with a slower one, plasma condenses, and a jump in the SW dynamic pressure P_{SW} is formed, which causes the magnetopause to rapidly approach Earth. Figure 2, *b* exhibits two steps of P_{SW}: from 1 to 5 nPa at 13:30 UT and to 20 nPa at 16 UT. Simultaneously with the last jump in P_{SW}, sharp variations in IMF occur, with B_z<–30 nT (Figure 2, *c*).

As a result, a magnetic storm develops with minimum *Dst*=–270 nT (Figure 2, *d*), the auroral electron flux increases significantly, and the auroral oval equatorial boundary shifts to lower latitudes. The maximum shift takes place in the near-midnight sector (at the longitude of the Northern Railway, it is 20–21 UT). In this longitude sector, the region of intense electron precipitation with energies 30 eV – 30 keV extends to latitudes from 70° to 52°, which leads to the fact that the SHO–LTO segment of the Northern Railway enters the zone of intense precipitation (Figure 2, *g*).

Location of the magnetic station Karpogory and stopping points on the Northern and October railways.

Station name	Code	Purpose	Geographic coordinates		Geomagnetic (CGM) coordinates		Universal Time of local magnetic midnight
			latitude	longitude	latitude, Φ	longitude, Λ	
Karpogory	KPG	IZMIRAN magnetic station IZMIRAN	64.0	44.5	60.0	120.8	20:33
Letneozersky	LTO	Northern Railway	63.4	40.3	59.5	116.9	20:26
Shestiozersky	SHO	Northern Railway	61.8	40.2	57.9	116.3	20:30
Murmansk	MMK	October Railway	69.0	33.1	65.3	113.8	20:38
Olenegorsk	OLN	October Railway	68.1	33.3	64.4	113.4	20:40
Apatity	APA	October Railway	67.6	33.4	63.8	113.1	20:41
Kandalaksha	KND	October Railway	67.2	32.4	63.5	112.1	20:45
Belomorsk	BLM	October Railway	64.5	34.8	60.8	112.6	20:43
Segezha	SGZ	October Railway	63.7	34.3	60.0	111.8	20:46
Medvezhay Gora	MDG	October Railway	62.9	34.4	59.2	111.6	20:47

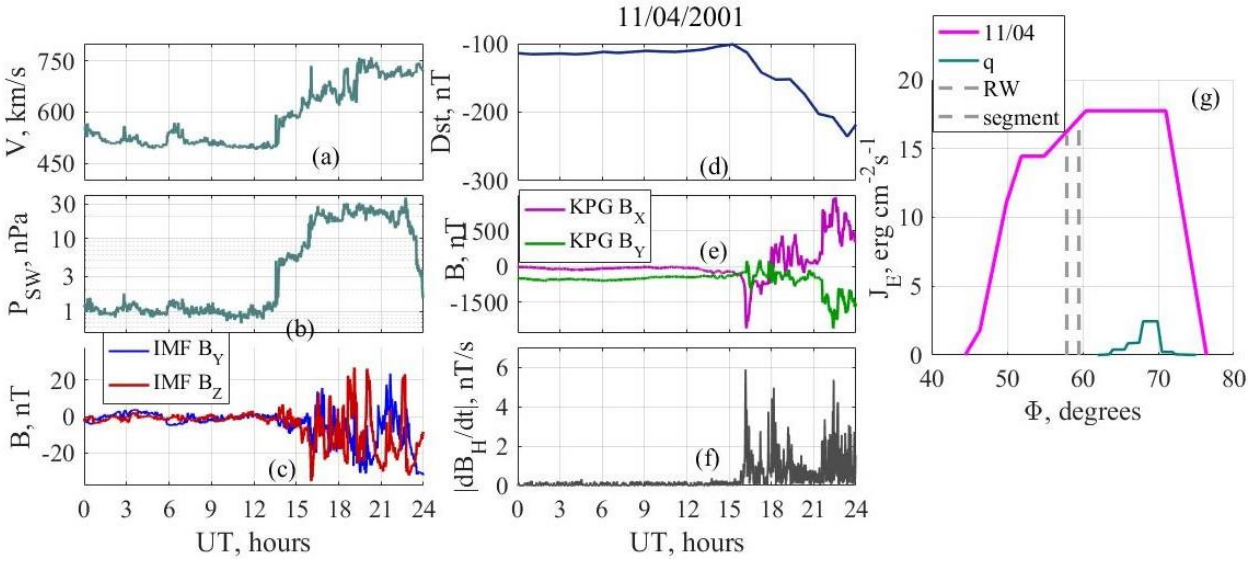

Figure 2. Interplanetary medium parameters, geomagnetic disturbances, and auroral precipitation on April 11, 2001: SW velocity V (*a*) and dynamic pressure P_{SW} (*b*), IMF components B_y, B_z (*c*), *Dst* index (*d*), variations in the geomagnetic field horizontal components B_x, B_y at the station Karpogory (*e*), and the modulus of the time derivative of the geomagnetic field horizontal component $|\Delta B_H/dt|$ (*f*), as well as distributions of precipitating auroral electron energy flux J_E along the geomagnetic latitude Φ at 20:30 UT on April 11, 2001 and on the next quiet day (q) according to [Vorobjev et al., 2013] (*g*); vertical dashed lines indicate latitudinal boundaries of a segment on the Northern Railway

Intense disturbances at the station Karpogory begin at ~16 UT with a negative bay having an amplitude ~2000 nT in the geomagnetic field meridional B_x component and irregular pulsations with a peak-to-peak amplitude of several hundred nanotesla in both horizontal components (Figure 2, *e*). The modulus of the time derivative of the magnetic field horizontal component $|dB_H/dt|$ exceeds 5 nT/s (Figure 2, *f*), which is much higher than the threshold of potentially dangerous disturbances [Viljanen et al., 2001].

The November 7–9, 2004 storm belongs to the so-called superstorms. Increased geomagnetic activity has been recorded for a long time at all latitudes [Manninen et al., 2008], and the most intense disturbances occur in auroral precipitation zones. Figure 3 shows the same interplanetary medium parameters as in Figure 2 for the period from 6 UT on November 7 to the end of the day on November 9. The storm starts with a sharp increase in the SW velocity and dynamic pressure at ~18 UT (Figure 3, *a*, *b*). At the same time, there are intense IMF variations (Figure 3, *c*) with minimum B_z=–50 nT. The initial phase of the storm features a sharp positive increase in *Dst* to +50 nT and a subsequent decrease to a minimum value of *Dst* =–374 nT at 7 UT on November 8 (Figure 3, *d*). Then, the recovery phase begins which is interrupted by a new "step" in the SW pressure and velocity at ~10 UT on November 9, and hence the *Dst* index, which has recovered to –120 nT by this time, falls below –200 nT again, and the second minimum *Dst*=–263 nT is observed on November 10. Note that both main *Dst* minima are caused by several solar wind disturbances (Figure 3, *a*–*c*), which leads to additional steps in *Dst* variations (Figure 3, *d*) and multiple auroral activations (Figure 3, *e*) from 18 UT on November 7 to 6 UT on November 8 and at the end of the day on November 9.

As a result, $|dB_H/dt|$ proves to be even higher than during the 2001 storm, reaching 6.5 nT/s, with two peaks recorded at night on November 7/8 and in the late evening–night on November 9 (Figure 3, *e*). Distribution of auroral precipitation for three days of this storm is illustrated for the midnight sector in Figure 3, *f*. On all the three days, the Northern Railway segment under study is in the zone of intense auroral precipitation. At the same time, the absolute values of J_E are slightly lower than those for the 2001 storm, a maximum of 14 erg cm^{-2} s^{-1}. The maximum flux level is recorded on November 8 during the recovery phase after the first *Dst* minimum. The distributions in Figure 3, *f* correspond to 23 UT when *Dst* recovered to –120 nT. In this case, both the precipitation intensity and the equatorial displacement of the precipitation zone are greater than those on November 7. On November 9, the precipitation intensity decreases to ~8 erg cm^{-2} s^{-1}, and the equatorial displacement of the precipitation zone reaches a maximum. As a result, the region of interest fell not on the low-latitude slope of the distribution, but on its maximum.

During this storm, failures were also observed on the Belomorsk segment of the October Railway. For example, on November 9 in the dawn sector from 9 to 11 local time (6–8 UT), false block occupancy of the railway circuit was recorded near the Shpalovaya stopping point (63.7° geographic latitude, Φ=60°).

Thus, the disturbances during the November 7–9 storm are characterized by high values of $|dB_H/dt|$ in the auroral precipitation zone, which covers geomagnetic latitudes to ~50°, and maximum values of $|dB_H/dt|$ are close during the main and recovery phases of the storm. The arrival of SW disturbance in the recovery phase leads to a second minimum of *Dst* and enhances the observed effects.

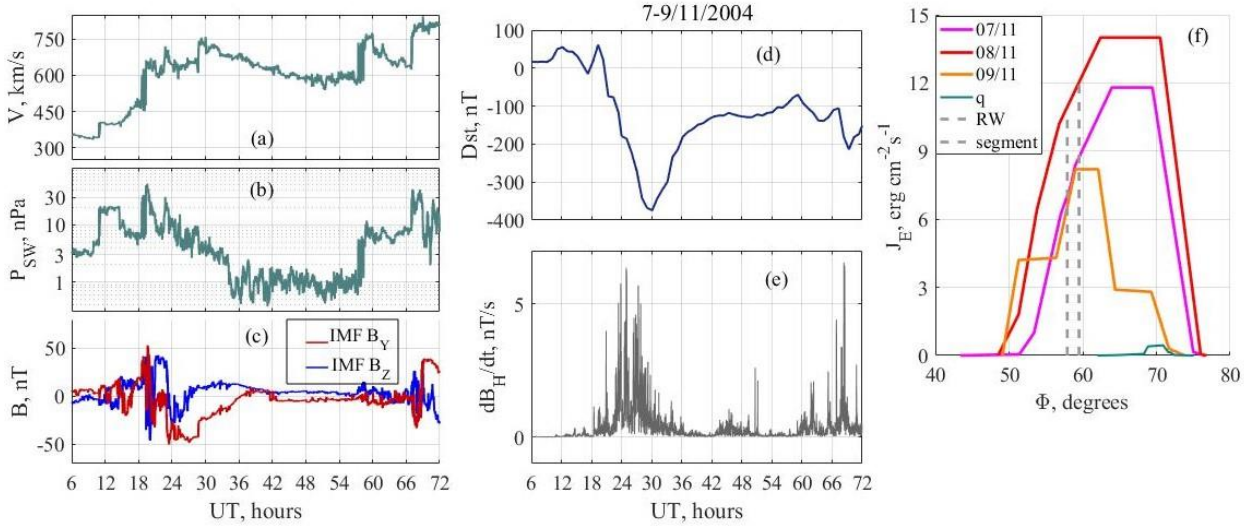

Figure 3. Interplanetary medium parameters, geomagnetic disturbances, and auroral precipitation on November 7–9, 2004: SW velocity *V* (*a*) and dynamic pressure P_{SW} (*b*); IMF components B_y, B_z (*c*); *Dst* index (*d*), and modulus of the time derivative of the geomagnetic field horizontal component $|\Delta B_H/dt|$ (*e*); zero time reference (*a*–*e*) is 0 UT on November 07, 2004. Also shown are distributions of the precipitating auroral electron energy flux J_E along the geomagnetic latitude Φ in the midnight sector for three days of the storm and on the next quiet day (*f*); vertical dashed lines are latitudinal boundaries of the Northern Railway segment

The November 20–21, 2003 storm is also a superstorm [Kleimenova et al., 2005]. It began with a jump in the SW velocity and dynamic pressure at ~8 UT on November 20 (Figure 4, *a*, *b*). The most intense oscillations of P_{SW} and IMF were detected till 17 UT, with single steps of P_{SW} reaching 20 nT, and the minimum value of B_z=–50 nT (Figure 4, *b*, *c*). As a result, a storm develops with minimum *Dst*=–422 nT at 21 UT (Figure 4, *d*). Local geomagnetic activity begins to increase from 9 UT simultaneously with intense IMF and P_{SW} disturbances. Maximum $|dB_H/dt|$ of ~7 nT/s is recorded at 14–18 and 22–23 UT (Figure 4, *e*). The maximum intensity of J_E is 13 erg cm^{-2} s^{-1}. The equatorial displacement of the precipitation zone is more pronounced than in all the events considered: the low-latitude boundary is below Φ=46° (Figure 4, *e*). Consequently, the region where failures on the Northern Railway were detected enters the zone of maximum precipitation intensity.

For this storm, numerous failures without apparent external cause were also recorded on the Belomorsk segment of the October Railway in 59.3°<Φ<60.8°. The failures were observed on November 20–25, i.e. until the end of the storm recovery phase, on 16 stages of the October Railway.

In all the cases related to the magnetic storm main and recovery phases, we have analyzed, failures in automatics were detected at subauroral geomagnetic latitudes.

2.2. Statistical regularities

Strong magnetic storms are the most dangerous sources of failures. However, such events are rare, so failures caused by moderate geomagnetic disturbances make a significant contribution to the general statistics. The availability of an archive of failures on two segments of the October Railway for five years — from 2002 to 2006 — allows us to statistically estimate the relationship between the spatial distribution of failures and the auroral oval position. The total number of failures for the five years was about 1800 on the Murmansk segment and 1300 on the Belomorsk segment.

In [Vorobjev et al., 2000, Vorobjev, Yagodkina, 2005; Vorobjev et al., 2013], spatial distributions of precipitating electrons in a limited local time interval are studied. For statistical estimation, it is advisable to use a parameter characterizing the position of the oval equatorial boundary for an arbitrary time; therefore, we employ the approximation [Holzworth, Meng, 1975] of the model [Feldstein, 1963] for the geomagnetic latitude of the oval equatorial boundary Φ_{aur}.

Since the archive of failures is not available for a continuous railway segment, but for two separate ones, and the classification of failures on them is not unified, we will analyze the oval equatorial boundary position during failures separately for the Murmansk (auroral) and Belomorsk (subauroral) segments. Following the method from [Yagova et al., 2023], of all failures we have identified failures of group 0 for which there is no obvious mechanical, meteorological, or anthropogenic cause.

The results are presented in Figure 5 as a dependence of $P(\Phi_{aur}<\Phi_b)$ on Φ_b, where *P* is the probability of passing through the oval boundary Φ_{aur} during a failure below the geomagnetic latitude Φ_b. Both for all failures (Figure 5, *a*) and for group 0 failures (Figure 5, *b*), the curve runs lower at the time when failures were recorded on the lower-latitude Belomorsk segment. This suggests that the latitudinal distribution of failures depends on the position of the oval equatorial boundary.

The assumption of the same distribution of Φ_{aur} for the time periods when failures were observed on the auroral (Murmansk) and subauroral (Belomorsk) segments of the October Railway was taken as the null hypothesis. To test this hypothesis, we have performed tests, using nonparametric criteria for both independent (Mann—Whitney) and dependent (Wilcoxon) readings [Kobzar, 2006], allowing conclusions to be drawn

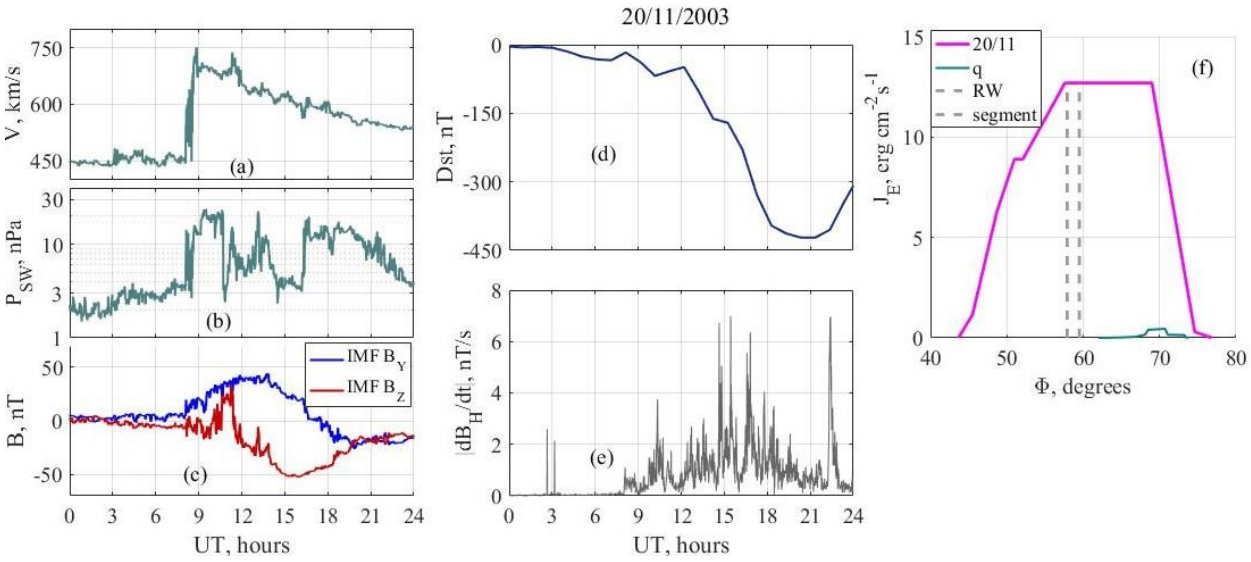

Figure 4. Interplanetary medium parameters, geomagnetic disturbances, and auroral precipitation on November 20, 2003 Designations are the same as in Figure 3

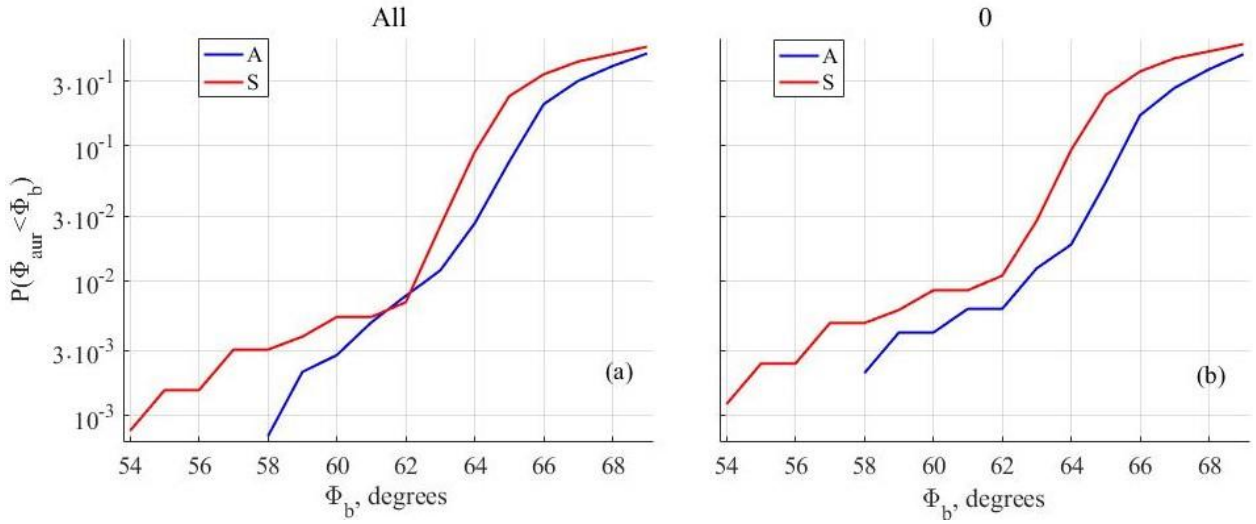

Figure 5. Probability that the oval equatorial boundary Φ_{aur} passes below the given geomagnetic latitude Φ_b during failures on the Murmansk (auroral, A) and Belomorsk (subauroral, S) segments of the October Railway: all failures (*a*); failures without an obvious external cause (group 0) (*b*)

about the equality or inequality of distributions in these sets. The Mann—Whitney criterion determines whether the zone of overlapping values between two sets is small enough (ranked subsets in the first sample and the same subset in the second sample). The lower the criterion, the more likely that the differences between the parameter values in the samples are significant. The Wilcoxon criterion is a nonparametric statistical test (criterion) used to test differences between two samples of paired or independent measurements by the level of any quantitative feature measured on a continuous or ordinal scale. The Wilcoxon test is performed by ranking the values in each sample, then calculating the sum of the ranks for each sample. To do the Wilcoxon test, the number of readings in two datasets was equalized by creating random samples of a dataset of superior length. The analysis has been carried out from five samples.

The analysis has shown that the null hypothesis can be rejected with a significance level of 5 % according to the Mann—Whitney criterion and 1 % according to the Wilcoxon criterion. Thus, the relative frequency of failures on the auroral and subauroral railway segments depends on the latitude of the auroral oval equatorial boundary. Moderate disturbances are the most dangerous for auroral segments. For more intense disturbances, the probability of failures at auroral latitudes decreases; and the high-risk zone descends to subauroral latitudes.

DISCUSSION

We have analyzed the latitudinal distribution of precipitation intensity, the auroral oval equatorial boundary position, and the modulus of the time derivative of geomagnetic field horizontal component $|dB_H/dt|$ at the Karpogory station during strong magnetic storms, for which an increase in the duration of failures in railway automatics was recorded [Eroshenko et al., 2010]. Under quiet conditions, the Northern Railway segment of interest is at subauroral latitudes. During all the storms considered, this segment was in the region of intense auroral precipitation, and maximum daily $|dB_H/dt|$ exceeded 5 nT/s. For the 2003 and 2004 superstorms, failures were also recorded on the subauroral (Belomorsk) segment of the October Railway (for the 2001 storm there was no available data on failures on the October Railway). Dangerous levels of disturbances occurred during both the main and recovery phases of the storm.

Statistical analysis of data from the archive of failures on two October Railway segments has confirmed the relationship between the position of the auroral oval equatorial boundary and the spatial distribution of failures. On days when failures were observed on the lower-latitude Belomorsk segment, a significant displacement to the south of the oval equatorial boundary was recorded. This effect was most pronounced during the strongest disturbances leading to the maximum displacement of the oval equatorial boundary: at $\Phi_{aur}<55°$, the vast majority of failures were detected at subauroral latitudes.

The resulting effect is weakly dependent on the type of failure indicated in the primary records. Possible causes of this may be related not only to the inaccurate initial classification or the indirect influence of space weather disturbances through meteorological and biological factors, as suggested in [Yagova et al., 2023]. On electrified railways, part of current is returned via a railway circuit. Both when using an impedance bond and a scheme with a continuous welded rail, quasi-static GICs can cause failures in automatics responsible for block occupancy [Patterson et al., 2023a, b]. The degree of this effect depends on the asymmetry of the circuit [Qian et al., 2016; Kostrominov, Lozhkin, 2021]. Since a change in the rail resistance or, more generally, the entire rail–ballast–ground system affects the balance of the current circuit, a situation arises when a change in resistance caused by human activity or weather conditions can exist for a long time without consequences, but manifests itself as a failure during a magnetic disturbance.

CONCLUSIONS

1. During strong magnetic storms of solar cycle 23, numerous failures were recorded on segments of the Northern and October railways, located at geomagnetic latitudes below 60°, where there was intense electron precipitation with energies to 30 keV with an energy flux above 7 erg cm^{-2} s^{-1}, and local geomagnetic activity exceeded 5 nT/s.

2. There is a statistically significant relationship between the geomagnetic latitude of the auroral oval equatorial boundary Φ_{aur} and the relative rate of failures on the auroral (Murmansk) and subauroral (Belomorsk) segments of the October Railway: during intense disturbances leading to a significant displacement of Φ_{aur} to the south, the proportion of failures on the subauroral segment increases.

3. The low-latitude boundary of the zone in which GIC-induced failures in railway automatics occur during geomagnetic disturbances can be approximately estimated by the latitude of the auroral oval equatorial boundary. More accurate estimates allowing for technical decision making require long-term data on failures on a particular railway.

The work was financially supported by RSF Grant No. 21-77-30010.

REFERENCES

Akasofu S.I. Interplanetary energy flux associated with magnetospheric substorms. *Planet. Space Sci*. 1979, vol. 27, pp. 425–431.

Beggan C. Sensitivity of geomagnetically induced currents to varying auroral electrojet and conductivity models. *Earth Planet Space*. 2015, vol. 67, 24. DOI: 10.1186/s40623-014-0168-9.

Boteler D.H. Modeling geomagnetic interference on railway signaling track circuits. *Space Weather*. 2021, vol. 19, e2020SW002609. DOI: 10.1029/2020SW002609.

Chisham G., Burrell A.G., Thomas E.G., Chen Y.-J. Ionospheric boundaries derived from auroral images. *J. Geophys. Res.: Space Phys*. 2022, vol. 127, e2022JA030622. DOI: 10.1029/2022JA030622.

Eroshenko E.A., Belov A.V., Boteler D., Gaidash S.P., Lobkov S.L., Pirjola R., Trichtchenko L. Effects of strong geomagnetic storms on Northern railways in Russia. *Adv. Space Res*. 2010, vol. 46, pp. 1102–1110. DOI: 10.1016/j.asr.2010.05.017.

Feldstein Y.I. On morphology and auroral and magnetic disturbances at high latitudes. *Geomagnetism and Aeronomy*. 1963, vol. 3, pp. 138–149.

Holzworth R.H., Meng C.-I. Mathematical representation of the auroral oval. *Geophys. Res. Lett*. 1975, vol. 2, pp. 377–380. DOI: 10.1029/GL002i009p00377.

Hu Z.-J., Yang Q.-J., Liang J.-M., Hu H.-Q., Zhang B.-C., Yang H.-G. Variation and modeling of ultraviolet auroral oval boundaries associated with interplanetary and geomagnetic parameters. *Space Weather*. 2017, vol. 15, pp. 606–622. DOI: 10.1002/2016SW001530.

Hu Z.-J., Han B., Zhang Y., Lian H., Wang P., Li G., et al. Modeling of ultraviolet aurora intensity associated with interplanetary and geomagnetic parameters based on neural networks. *Space Weather*. 2021, vol. 19, e2021SW002751. DOI: 10.1029/2021SW002751.

Kasinskii V.V., Lyahov N.N., Ptitsyna N.G., Tyasto M.I., Villoresi G., Iucci N. Effect of geomagnetic disturbances on the operation of railroad automated mechanics and telemechanics. *Geomagnetism and Aeronomy*. 2007, vol. 47, pp. 676–680.

Kleimenova N.G., Kozyreva O.V., Manninen J., Ranta A. Unusual strong quasi-monochromatic ground Pc5 geomagnetic pulsations in the recovery phase of November 2003 superstorm. *Ann. Geophys*. 2005, vol. 23, pp. 2621–2634. DOI: 10.5194/angeo-23-2621-2005.

Kobzar A.I. *Prikladnaya matematicheskaya statistika* [Applied Mathematical Statistics]. Moscow, Fizmatlit Publ., 2006, 816 p. (In Russian).

Kostrominov A.M., Lozhkin R.O. Influence of geoinduced currents on impedance bonds with secondary windings used in railway automation circuits. [*Izvestiya Peterburgskogo universiteta putei soobshcheniya*] [Proceedings of Petersburg Transport University]. 2021, vol. 18, pp. 222–228. DOI: 10.20295/1815-588X-2021-2-222-228. (In Russian).

Love J.J., Hayakawa H., Cliver E.W. Intensity and impact of the New York Railroad superstorm of May 1921. *Space Weather*. 2019, vol. 17, pp. 1281–1292. DOI: 10.1029/2019SW002250.

Manninen J., Kleimenova N.G., Kozyreva O.V., Ranta A., Kauristie K., Mäkinen S., Kornilova T.A. Ground-based observations during the period between two strong November 2004 storms attributed to steady magnetospheric convection. *J. Geophys. Res*. 2008, vol. 113, A00A09. DOI: 10.1029/2007JA 012984.

Milan S.E. Both solar wind-magnetosphere coupling and ring current intensity control of the size of the auroral oval. *Geophys. Res. Lett*. 2009, vol. 36, L18101. DOI: 10.1029/2009GL039997.

Newell P.T., Sotirelis T., Ruohoniemi J.M., Carbary J.F., Liou K., Skura J.P., Meng C.-I., Deehr C., Wilkinson D., Rich F.J. OVATION: Oval variation, assessment, tracking, intensity, and online nowcasting. *Ann. Geophys*. 2002, vol. 20, pp. 1039–1047. DOI: 10.5194/angeo-20-1039-2002.

Ohma A., Laundal K.M., Madelaire M., Hatch S.M., Gasparini S., Reistad J.P., et al. Robust estimates of spatiotemporal variations in the auroral boundaries derived from global UV imaging. *J. Geophys. Res.: Space Phys*. 2024, vol. 129, e2023JA032021. DOI: 10.1029/2023JA032021.

Patterson C.J., Wild J.A., Boteler D.H. Modeling the impact of geomagnetically induced currents on electrified railway signaling systems in the United Kingdom. *Space Weather*. 2023a, vol. 21, e2022SW003385. DOI: 10.1029/2022SW003385.

Patterson C.J., Wild J.A., Boteler D.H. Modeling "wrong side" failures caused by geomagnetically induced currents in electrified railway signaling systems in the UK. *Space Weather*. 2023b, vol. 21, e2023SW003625. DOI: 10.1029/2023SW003625.

Pilipenko V.A., Chernikov A.A., Soloviev A.A., Yagova N.V., Sakharov Ya.A., Kostarev D.V., et al. Influence of space weather on the reliability of the transport system functioning at high latitudes. *Russian Journal of Earth Sciences*. 2023, vol. 23, ES2008. DOI: 10.2205/2023 ES000824. (In Russian).

Ptitsyna N.G., Kasinskii V.V., Villoresi G., Lyahov N.N., Dorman L.I., Iucci N. Geomagnetic effects on mid-latitude railways: A statistical study of anomalies in the operation of signaling and train control equipment on the East-Siberian Railway. *Adv. Space Res*. 2008, vol. 42, pp. 1510–514. DOI: 10.1016/j.asr. 2007.10.015.

Qian X., Tian H., Yin Y., Li Y., Liu M., Jiang Z. Geomagnetic Storms' Influence on Intercity Railway Track Circuit. *Urban Rail Transit*. 2016, vol. 2, pp. 85–91. DOI: 10.1007/s40864-016-0040-2.

Sakharov Y.A., Yagova N.V., Pilipenko V.A. Pc5/Pi3 geomagnetic pulsations and geomagnetically induced currents. *Bull. Russian Acad. Sci. Phys*. 2021, vol. 85, pp. 329–333. DOI: 10.3103/S1062873821030217.

Viljanen A., Nevanlinna H., Pajunpaa K., Pulkkinen A. Time derivative of the horizontal geomagnetic field as an ac-

tivity indicator. *Ann. Geophys*. 2001, vol. 19, pp. 1107–1118. DOI: 10.5194/angeo-19-1107-2001.

Viljanen A., Tanskanen E.I., Pulkkinen A. Relation between substorm characteristics and rapid temporal variations of the ground magnetic field. *Ann. Geophys*. 2006, vol. 24, pp. 725–733. DOI: 10.5194/angeo-24-725-2006.

Vorobjev V.G., Rezhenov B.V., Starkov G.V., Gromova L.I., Feldstein Ya.I. Variations of the boundaries of plasma precipitation and auroral luminosity in the nighttime sector. *Geomagnetism and Aeronomy*. 2000, vol. 40, pp. 344–350.

Vorobjev V.G., Yagodkina O.I. Effect of geomagnetic activity on the global distribution of auroral precipitation zones. *Geomagnetism and Aeronomy*. 2005, vol. 45, pp. 438–444.

Vorobjev V.G., Yagodkina O.I., Katkalov Y. Auroral precipitation model and its applications to ionospheric and magnetospheric studies. *J. Atmos. Solar-Terr. Phys*. 2013, vol. 102, pp. 157–171. DOI: 10.1016/j.jastp.2013.05.007.

Wik M., Viljanen A., Pirjola R., Pulkkinen A., Wintoft P., Lundstedt H. Calculation of geomagnetically induced currents in the 400 kV power grid in Southern Sweden. *Space Weather*. 2008, vol. 6, S07005. DOI: 10.1029/2007SW000343.

Wik M., Pirjola R., Lundstedt H., Viljanen A., Wintoft P., Pulkkinen A. Space weather events in July 1982 and October 2003 and the effects of geomagnetically induced currents on Swedish technical systems. *Ann. Geophys*. 2009, vol. 27, pp. 1775–1787. DOI: 10.5194/angeo-27-1775-2009.

Wintoft P., Viljanen A., Wik M. Extreme value analysis of the time derivative of the horizontal magnetic field and computed electric field. *Ann. Geophys*. 2016, vol. 34, pp. 485–491. DOI: 10.5194/angeo-34-485-2016.

Yagova N.V., Rozenberg I.N., Gvishiani A.D., Sakharov Ya.A., Garanin S.L., Voronin V.A., et al. Study of geomagnetic activity impact on functioning of railway automatics in Russian Arctic. *Arktika: ekologiya I ekonomika* [Arctic: Ecology and Economy]. 2023, vol. 13, pp. 341–352. DOI: 10.25283/2223-4594-2023-3-341-352. (In Russian).

Original Russian version: Sakharov Ya.A., Yagova N.V., Pilipenko V.A., Yagodkina O.I., Garanin S.L., published in Solnechno-zemnaya fizika. 2024. Vol. 10. No. 4. P. 114–121. DOI: 10.12737/szf-104202412.

How to cite this article

Sakharov Ya.A., Yagova N.V., Pilipenko V.A., Yagodkina O.I., Garanin S.L. Spatial distribution of auroral precipitation and failures in railway automatics at the north of European Russia. *Solar-Terrestrial Physics*. 2024. Vol. 10. Iss. 4. P. 106–113. DOI: 10.12737/stp-104202412.